

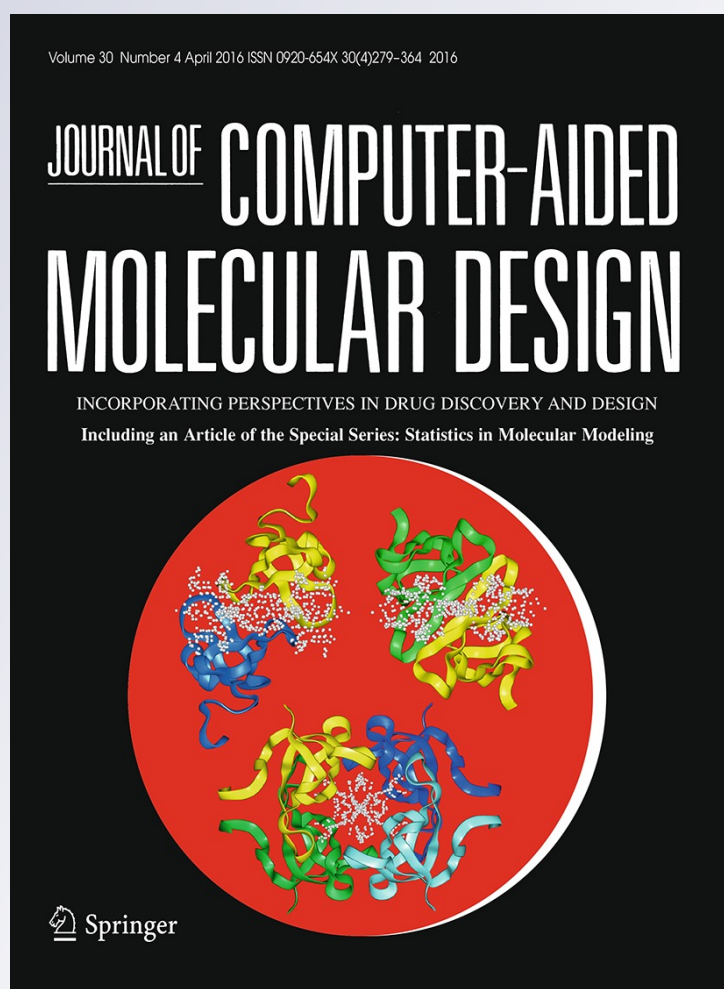
Discovery of novel polyamine analogs with anti-protozoal activity by computer guided drug repositioning

**Lucas N. Alberca, María L. Sbaraglini,
Darío Balcazar, Laura Fraccaroli,
Carolina Carrillo, Andrea Medeiros,
Diego Benitez, et al.**

**Journal of Computer-Aided
Molecular Design**
Incorporating Perspectives in Drug
Discovery and Design


ISSN 0920-654X
Volume 30
Number 4

J Comput Aided Mol Des (2016)
30:305-321
DOI 10.1007/s10822-016-9903-6



Your article is protected by copyright and all rights are held exclusively by Springer International Publishing Switzerland. This e-offprint is for personal use only and shall not be self-archived in electronic repositories. If you wish to self-archive your article, please use the accepted manuscript version for posting on your own website. You may further deposit the accepted manuscript version in any repository, provided it is only made publicly available 12 months after official publication or later and provided acknowledgement is given to the original source of publication and a link is inserted to the published article on Springer's website. The link must be accompanied by the following text: "The final publication is available at link.springer.com".

Discovery of novel polyamine analogs with anti-protozoal activity by computer guided drug repositioning

Lucas N. Alberca¹ · María L. Sbaraglini¹ · Darío Balcazar² ·
Laura Fraccaroli² · Carolina Carrillo² · Andrea Medeiros³ ·
Diego Benitez³ · Marcelo Comini³ · Alan Talevi¹ 

Received: 20 November 2015 / Accepted: 12 February 2016 / Published online: 18 February 2016
© Springer International Publishing Switzerland 2016

Abstract Chagas disease is a parasitic infection caused by the protozoa *Trypanosoma cruzi* that affects about 6 million people in Latin America. Despite its sanitary importance, there are currently only two drugs available for treatment: benznidazole and nifurtimox, both exhibiting serious adverse effects and limited efficacy in the chronic stage of the disease. Polyamines are ubiquitous to all living organisms where they participate in multiple basic functions such as biosynthesis of nucleic acids and proteins, proliferation and cell differentiation. *T. cruzi* is auxotroph for polyamines, which are taken up from the extracellular medium by efficient transporters and, to a large extent, incorporated into trypanothione (bis-glutathionylspermidine), the major redox cosubstrate of trypanosomatids. From a 268-compound database containing polyamine analogs with and without inhibitory effect on *T. cruzi* we have inferred classificatory models that were later applied in a virtual screening campaign to identify anti-trypanosomal compounds among drugs already used for other

therapeutic indications (i.e. computer-guided drug repositioning) compiled in the DrugBank and Sweetlead databases. Five of the candidates identified with this strategy were evaluated in cellular models from different pathogenic trypanosomatids (*T. cruzi wt*, *T. cruzi PAT12*, *T. brucei* and *Leishmania infantum*), and in vitro models of aminoacid/polyamine transport assays and trypanothione synthetase inhibition assay. Triclabendazole, sertaconazole and paroxetine displayed inhibitory effects on the proliferation of *T. cruzi* (epimastigotes) and the uptake of putrescine by the parasite. They also interfered with the uptake of others aminoacids and the proliferation of infective *T. brucei* and *L. infantum* (promastigotes). Trypanothione synthetase was ruled out as molecular target for the anti-parasitic activity of these compounds.

Keywords Chagas disease · Drug repositioning · Polyamines · *Trypanosomatids* virtual screening · Paroxetine · Triclabendazole

Electronic supplementary material The online version of this article (doi:10.1007/s10822-016-9903-6) contains supplementary material, which is available to authorized users.

✉ Alan Talevi
atalevi@biol.unlp.edu.ar

¹ Laboratory of Bioactive Compounds Research and Development (LIDeB), Medicinal Chemistry, Department of Biological Science, Exact Sciences College, National University of La Plata (UNLP), Argentina, 47 & 115, B1900AJI La Plata, Buenos Aires, Argentina

² Instituto de Ciencias y Tecnología Dr. César Milstein (ICT Milstein), Argentinean National Council of Scientific and Technical Research (CONICET), Buenos Aires, Argentina

³ Laboratory Redox Biology of Trypanosomes, Institut Pasteur de Montevideo, 11400 Montevideo, Uruguay

Introduction

Chagas disease is an endemic parasitic disease of Latin America caused by the flagellate protozoan *Trypanosoma cruzi*. The main route of transmission of the pathogen is through the bite of the vector insect. Other less common routes of infection include congenital transmission, blood transfusion, ingestion of contaminated food and laboratory accidents [1, 2]. The human disease presents two stages: an acute stage, taking place shortly after infection, and a chronic stage that develops years to decades later. The acute phase usually goes undetected because it lacks specific symptoms. The lifelong chronic stage commonly remains asymptomatic, though about 30 % of the patients

develop pathologies affecting the heart, the digestive or the nervous system. About two-thirds of people with chronic symptoms undergo lethal cardiac damage; one-third develops digestive system damage, resulting in megacolon and/or megaesophagus, accompanied by severe weight loss [3, 4]. According to data from the World Health Organization, 6–7 million people are nowadays infected worldwide, mostly in Latin America [5]. Despite this figure and the steady advances in understanding the biology of *T. cruzi*, there are currently only two drugs available for the treatment of Chagas disease, namely benznidazole and nifurtimox. These medicines were discovered over 40 years ago, are ineffective in the chronic phase of the disease and present severe side-effects [6]. Although there is some controversy about the benefits of using benznidazole in the chronic stage, the recently published results of the Benznidazole Evaluation for Interrupting Trypanosomiasis (BENEFIT) study showed that treatment with benznidazole in adult chronic patients does not significantly reduce cardiac dysfunction through 5 years of follow-up [7], reaffirming the need for new drugs with improved efficacy and safety profile.

The polyamine based metabolism of trypanosomatids is an interesting pathway for drug development because these metabolites (putrescine, spermidine and spermine) play important roles in the biosynthesis of nucleic acids and proteins, in proliferation and cell differentiation, and in the protection against oxidative damage, which in these organisms depends on a bisglutathionyl conjugate of spermidine, called trypanothione, absent in mammals [8].

T. cruzi lacks the enzymes arginine decarboxylase and ornithine decarboxylase, which catalyze the first steps in polyamine biosynthesis (Fig. 1) [9, 10]. Therefore, it strictly depends on polyamine uptake (especially for putrescine) from the host cell [11]. The putrescine transporter TcPAT12 (also called TcPOT1.1/2, Accession Number: EU544169 or FJ204167, respectively) has been functionally characterized and shown to be almost exclusive of *T. cruzi* with no homologous in the mammalian

lineage, hence qualifying as an attractive drug target candidate [12, 13]. Polyamine transporters belong to the superfamily of transporters called AAAP (Amino Acid/Auxin Permeases), which transport essential amino acids for *T. cruzi*, suggesting that a non-selective inhibition of these transporters may result in an enhanced anti-parasitic activity due to the simultaneous impairment of several metabolic pathways dependent on indispensable aminoacids [14].

As pointed above, spermidine is essential for trypanosomatids because it is a building block of the main low molecular mass redox co-substrate of these organisms, trypanothione, that is pivotal for parasite survival. In this respect, the synthesis of trypanothione ($T(SH)_2$) by trypanothione synthetase (TRY5; Fig. 1) has also been shown to be essential in viability and maintenance in *Trypanosoma brucei* [15] and *Leishmania infantum* [16].

In recent years, drug repurposing (or drug repositioning) has become of great interest in the international pharmaceutical community. The strategy involves finding new therapeutic indications for approved, discontinued, shelved or even experimental drugs [17, 18]. This strategy has remarkable advantages over the search for de novo drugs: the cost and time required for the development of an innovative medication are greatly reduced, in part because both toxicological and pharmacokinetic profile of the repositioned drug have already been characterized when investigating the original therapeutic indication [19, 20]. There are many successful repurposing stories. For example, the anticonvulsant valproic acid is now also used for the treatment of bipolar disorder and migraines; in 2009, the antiparkinsonian bromocriptine has gained FDA approval as a treatment of type 2 diabetes; the traditional therapeutic indications of aspirin have some years back been expanded to the prevention of heart attack and stroke in cardiac patients; besides its use as a treatment for erectile dysfunction, sildenafil is now approved for its originally pursued indication: the treatment of pulmonary hypertension. It has been reported that drug repurposing

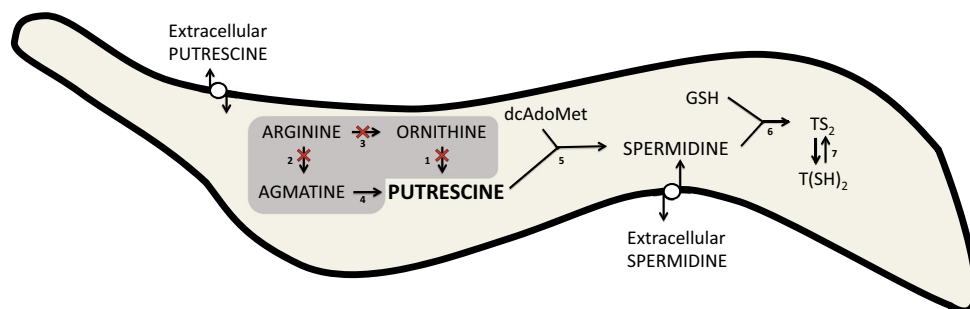


Fig. 1 Scheme of polyamine metabolism in *T. cruzi*. 1 ornithine decarboxylase, 2 arginine decarboxylase, 3 arginase, 4 agmatinase, 5 spermidine synthase, 6 trypanothione synthetase, 7 trypanothione

reductase. GSH, glutathione; dcAdoMet, S-adenosyl-L-methionine; $T(SH)_2$, reduced trypanothione; TS_2 , trypanothione disulfide (oxidized)

may be particularly useful for the discovery of new treatments for neglected diseases, such as Chagas disease [21]; in fact, most of the drug candidates at clinical stage for Leishmaniasis, Chagas disease and Human African Trypanosomiasis are repurposed drugs [22].

In this work, we present the development of computational models capable of recognizing polyamine analogs with activity towards *T. cruzi*. The best models have been combined through ensemble learning approaches and then applied in a virtual screening (VS) campaign focused in drug repositioning, in order to identify drugs with potential anti-trypanosomal activity. Five of the in silico selected candidates were assayed for their anti-*T. cruzi*, -*T. brucei* and -*L. infantum* activity and their inhibitory effect on putrescine uptake and trypanothione synthetase.

Materials and methods

Dataset compilation

We performed an extensive literature search of polyamine analogues that have been tested in proliferation assays against *T. cruzi*. We compiled a 268-compound (123 active compounds, 145 inactive compounds) database from different reports [23–43], in which a polyamine analog was defined as an active drug when presenting a half-maximal growth inhibition concentration (EC_{50}) below 20 μ M. Compounds with EC_{50} greater than 20 μ M were considered as non-inhibitors or “inactive”. The chemical structures of the compound dataset are presented as Supplementary Material A; their chemical diversity might be appreciated. A heatmap illustrating the molecular dissimilarity between the active and inactive compounds in the dataset was constructed using Gitools v. 2.2.3 [44]. Molecular dissimilarity was calculated with JChem v. 6 (ChemAxon, 2013), using ECFP_4 as fingerprinting system.

Splitting the dataset into training and test sets

We split the compound database into two sets of compounds: (a) a training set that was used to infer the models and; (b) an independent test set that served to assess the predictive ability of the generated models. In order to split the database into representative sets, we combined two clustering methodologies: first, a hierarchical clustering method using the LibraryMCS (ChemAxon) software, which relies on similarity-guided Maximum Common Substructure (MCS, i.e. the largest subgraph shared by two chemical graphs) to cluster a set of chemical structures without exhaustive pair wise comparison [45–48]. Subsequently, we optimized this

clustering through the k-means optimization algorithm implemented in Statistica 10 Cluster Analysis module (Statsoft, 2011). Ideally, the training set should present a balanced composition between active and inactive compounds to prevent a bias of the models towards predicting a particular category. For this reason, 75 % of each cluster of the active compounds and 63 % of each cluster of the inactive compounds were assigned to the training set, resulting in an equal number of active and inactive compounds in the calibration sample; the remaining compounds were used as test set.

Descriptor calculation

For molecular descriptor calculation we used Dragon 6.0 software (Milano Chemometrics, 2011), obtaining more than 3000 conformation-independent descriptors for each chemical compound in the dataset; since computing such descriptors does not require pre-optimization of the molecular structures, their calculation is time-efficient allowing exploration of large chemical libraries. For modeling purposes, the descriptor pool was randomly partitioned into 100 descriptor subsets with no more than 200 descriptors each and one model was obtained from each subset through a forward stepwise procedure (see next subsection). Such strategy for parallel model generation, which corresponds to a random subspace approach, serves a twofold purpose: it prospectively reduces the probability of finding chance correlations (which increases with the number of potential independent variables in the descriptor pool) while simultaneously allows a stochastic exploration of the feature space.

Modeling

The molecular descriptors that best correlate with the modeled dependent variable were selected using the linear discriminant analysis (LDA) module of Statistica 10 software, using a forward stepwise procedure. LDA is a learning method aimed to finding a linear combination of predictor variables to discriminate between two or more categories of objects. Each object class is associated to a given value of an arbitrary variable that serves as class label. In our case, two object classes (ACTIVE and INACTIVE) were considered; thus the class label assumes two observed values (1 and -1, respectively). LDA and other classificatory techniques may be useful to handle noisy data, e.g. if a given experimental endpoint is associated to large variability or if experimental data from a diversity of laboratories are compiled [49].

A tolerance value of 0.5 was selected in order to exclude highly correlated descriptors from the model. A minimum ratio of 15 between the number of training set examples

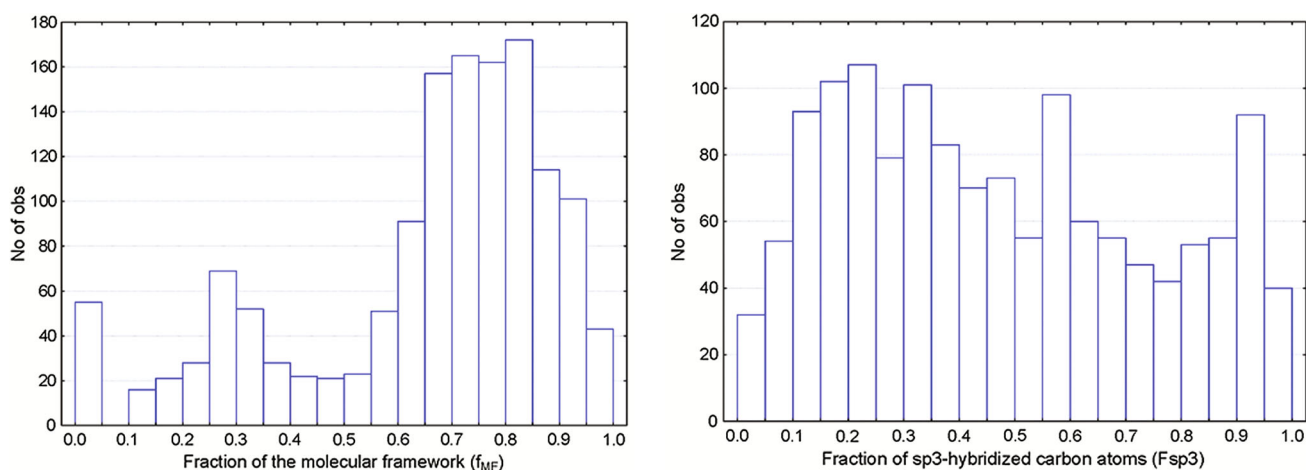


Fig. 2 Distribution of the topologies of the DUD-E decoys

and the number of independent variables was used in order to reduce the chance of overfitting; since the training set included a total of 184 training examples, no more than 12 descriptors were allowed into the model. All the coefficients linked to the models descriptors were significant at a 0.05 level. The performance of the models on the independent test set and the simulated database (see below) was used to select the best models.

Validation of models

Each generated model was validated by several conventional techniques: (a) internal validation using cross-validation and Fisher randomization test [50]; (b) external validation.

Subsequently, the performance of the models was tested in pilot campaigns of VS, dispersing the active compounds from the test set among a large number of presumed inactive compounds (decoys). These compounds were generated by two different methods. Initially, we took the 53 inactive compounds from the test set and search for PubChem compounds having 95 % of chemical similarity to the queries. We found 369 similar compounds by this methodology which were consider as decoys. We called this database “Simulated Database”.

Second, we have used the Enhanced Directory of Useful Decoys resource (DUD-E) to build a second, larger and more diverse chemical library (which was called “DUD-E Library”) containing 1475 compounds (1391 decoys plus the original 84-compound test set) where each decoy is physicochemically similar but topologically different to the corresponding active compound. For this purpose we used the automated decoy generation tool available online [51]. Shortly, the decoys are property-matched to the queries (in this case, the active compounds) using molecular weight,

an estimated log transformation of the octanol–water partition coefficient (mLogP), rotatable bonds, hydrogen bond donors and acceptors count and net molecular charge. All ligands protonation states in the pH range 6–8 are obtained using Schrödinger’s Epik with arguments “-ph 7.0 -pht 1.0 -tp 0.20”. About 50 decoys are generated for each ligand. To achieve this, a pool of decoys are selected from ZINC [52] using a dynamic protocol that adapts to the local chemical space by narrowing or widening windows around the 6 matched properties. The goal is to return 3000–9000 potential decoys matching the ligands. In a final step, ECFP4 fingerprints are generated by Scitegic’s Pipeline Pilot for the ligands and its potential decoys. The decoys are sorted by their Tanimoto coefficient to each ligand and the most dissimilar 25 % are kept. Figure 2 displays the fraction of the molecular framework and the fraction of sp³-hybridized carbon atoms; these two descriptors have previously been proposed to describe molecular topology by Yang et al. [53, 54].

Since the models will be used to define, in a database of thousands of compounds, which ones are most likely to possess the desired activity, it is important to establish a cut-off in the model response (score) associated with an adequate balance between sensitivity (Se, the rate of true positives, TP) and specificity (Sp, the true negative rate, TN):

$$Se = \frac{TP}{TP + FN} \quad Sp = \frac{TN}{TN + FP}$$

where FN denotes false negatives and FP represents false positives. For this purpose we have applied ROC curves (Receiving Operating Characteristic) analysis [55]: a perfect classifier presents an area under the ROC curve (AUROC) of 1, while random classification is associated to an AUROC of 0.5. MedCalc (MedCalc software, 2011) was used to obtain and statistically compare ROC curves.

The nonparametric method of DeLong et al. [56] was used to compare AUROCs from a statistical viewpoint.

Ensemble learning

Ensemble learning uses multiple learning algorithms to obtain better predictive performance than the performance that could be obtained from any of the individual constituent learning algorithms [57]. Here, we have combined the scores of the 6 individual models that showed the best AUCROC on the simulated database. We have used five combination schemes to obtain a combined score: MAX operator (which returns the maximum score among the individual scores of the combined models); MIN operator (which returns the minimum score among the individual scores of the combined models); Average Score; Average Ranking and Average Voting. Voting was computed according to the equation previously used by Zhang and Muegge [58]. The five combination schemes were analyzed and compared through ROC curve analysis.

Virtual screening

We screened two databases: (a) DrugBank 3.0, which compiles approved drugs for clinical use by the Food and Drug Administration of USA (FDA) and drugs in clinical evaluation stage [59]; (b) Sweetlead, which contains drugs approved by other international regulatory agencies, plus traditional medicine natural products [60].

Five compounds selected by the best combination of models were purchased for experimental evaluation.

Experimental assays

Biological activity towards trypanosomatids

For all assays, stock and working solutions of the test compounds were prepared using DMSO as solvent and test or control conditions were tested in triplicate.

Epimastigotes of the Y strain of *T. cruzi* were cultured at 28 °C in BHT medium supplemented with 20 mg/mL haemin, 10 % heat-inactivated fetal bovine serum (FBS), 100 µg/mL streptomycin and 100 U/mL penicillin. The antiproliferative activity of the compounds was tested at concentrations from 3 to 100 µM in cultures of 10⁷ cells/mL. After 4 and 8 days, the number of viable parasites were counted using a hemocytometer chamber under the light microscope [61].

Bloodstream form *T. brucei brucei* strain 427, cell line 449 [62], expressing a redox biosensor [Sardi and Comini, unpublished] was cultured in a humidified incubator at 37 °C with 5 % CO₂ in HMI-9 medium supplemented with 10 % (v/v) FBS, 10 U/mL penicillin, 10 µg/mL streptomycin,

0.2 µg/mL phleomycin, 5 µg/mL hygromycin and, eventually, 1 µg/mL oxytetracycline to induce the expression of the redox biosensor. Trypanosomes were grown to exponential phase and diluted at a cell density of 5 × 10⁵ cells/mL (mid exponential phase) in fresh culture medium. Two hundred µL of the cell suspension was plated into each well of a 96-well culture plate. Compounds were immediately added at final concentrations in the range of 0.1 and 25 µM. DMSO at 1 % (v/v) was included as growth control. After 24 h incubation; viable parasites were counted using a flow cytometer BD Accuri™ C6 and discriminating death from living parasites by propidium iodide staining (2 µg/mL).

L. infantum promastigotes (MHOM MA67ITMAP263) were cultured at 28 °C in RPMI 1640 Glutamax supplemented with 10 % (v/v) FBS, 10 U/mL penicillin, 10 µg/mL streptomycin and 25 mM HEPES sodium salt pH 7.4. Synchronized cultures were seeded at 5 × 10⁵ cells/mL in 96-well plates in complete RPMI medium with varying concentrations (0.2–5 µM) of compounds in 1 % (v/v) DMSO. Twenty-four hours later parasite viability was measured by cell counting under the light microscope using a Neubauer chamber and calculated as percentage in relation to control cultures incubated with the vehicle alone and with 0.02–0.03 mg/mL potassium antimonyl tartrate trihydrate as control drug.

For all assays described above, the EC₅₀ values were determined from dose response curves fitted to a sigmoidal equation (Boltzmann model) or extrapolated from linear fitting plots [63].

Aminoacid/Polyamine transport assay

Aliquots of *T. cruzi* epimastigotes (3 × 10⁷ parasites) grown for 24 h in a medium depleted from putrescine were centrifuged at 1500g for 10 min and washed three times with phosphate-buffered saline (PBS). The cells were then resuspended in 2 mL of PBS containing 5 µM (¹⁴C)-putrescine, or (¹⁴C) arginine, or (¹⁴C) lysine, or (¹⁴C) uridine, and the compounds at a concentration of 50 µM. Aliquots were taken at different times. These aliquots were centrifuged and washed twice with 1 mL of ice cold PBS and the corresponding labeled aminoacid at 10 mM. Pellets were resuspended and radioactivity determined in UltimaGold XR [23]. The test compounds were prepared using DMSO as solvent and final concentration of DMSO was 0.1 %. All experiments were performed in triplicate.

Moreover, the effect of the drug on parasite viability was evaluated through the tetrazolium salt (MTT) reduction assay [64]. Briefly, 10 µL of 5 mg/mL MTT dye (3[4,5-dimethylthiazol-2-yl]-2,5-diphenyltetrazolium bromide) was added to the eppendorf tubes containing 10⁶ parasites in 100 µL of BHT and the drug candidates 50 µM. After incubation for 3.5 h at 28 °C, the tubes

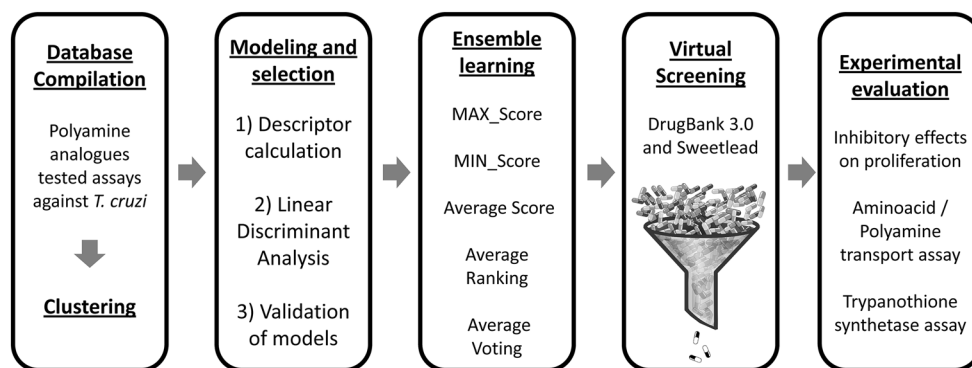
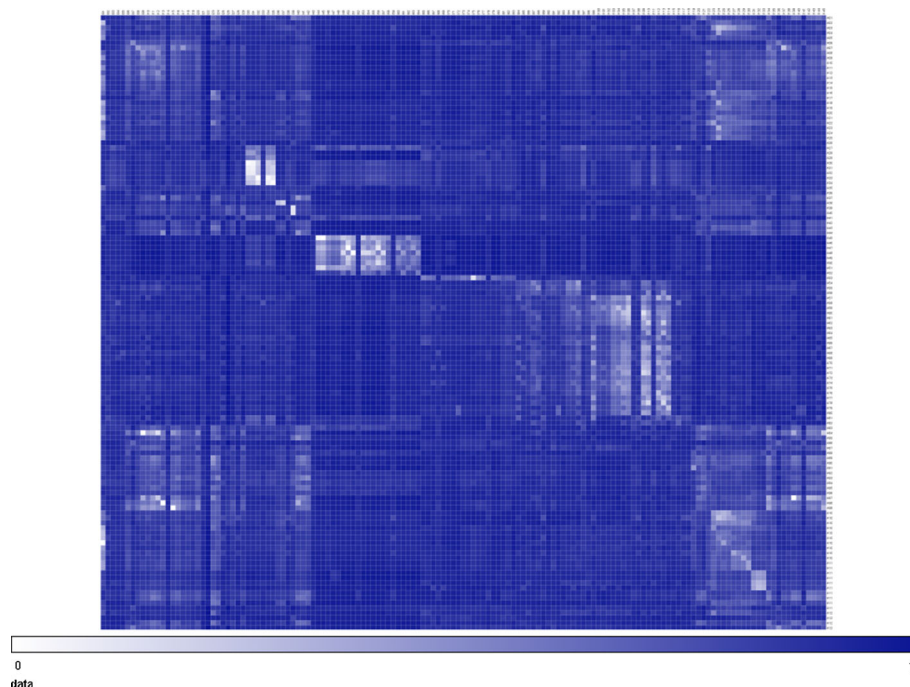


Fig. 3 Schematic representation of the screening and validation strategy

Fig. 4 Heatmap of dissimilarity of the active compounds versus inactive compounds of dataset



were spin-dry (3000 rpm) and the pellet with the formazan crystals were dissolved with 100 μL of 10 % (w/v) SDS in 0.01 M HCl. The optical density (OD) was determined using a microplate reader (Labsystems Multiskan MS, Finland) at 570 nm/695 nm. Under such conditions, the OD is proportional to the viable cell number in each well. All experiments were performed in triplicate.

Trypanothione synthetase enzymatic assay

Trypanothione synthetase (TryS) activity of *L. infantum* (LiTryS) and *T. brucei* (TbTryS) was determined using the malachite green reagent (BIOMOL GREENTM; Enzo Life Sciences) that allows measuring the amount of inorganic phosphate released from ATP during catalysis.

The assay was conducted at room temperature, using a 96-well plate and a total reaction volume of 50 μL per well: 40 μL of 100 mM HEPES-K potassium salt pH 7.4, 0.5 mM EDTA, 10 mM MgSO_4 , 5 mM DTT (reaction buffer), 2 mM spermidine, glutathione (250 μM for LiTryS and 50 μM for TbTryS), and 150 μM ATP. The concentrations of spermidine and glutathione in the reaction were fixed according to the intracellular levels reported in the literature and of the one of ATP was adjusted to avoid assay interference. We use 5 μL of LiTryS (final concentration 200 nM) or TbTryS (final concentration 200 nM) and 5 μL of inhibitor dissolved in DMSO or 5 μL of DMSO (control reaction). The reaction was initiated by adding the enzyme (or reaction buffer for the blanks) and stopped after 15 min with 200 μL of BIOMOL GREENTM. The colorimetric signal

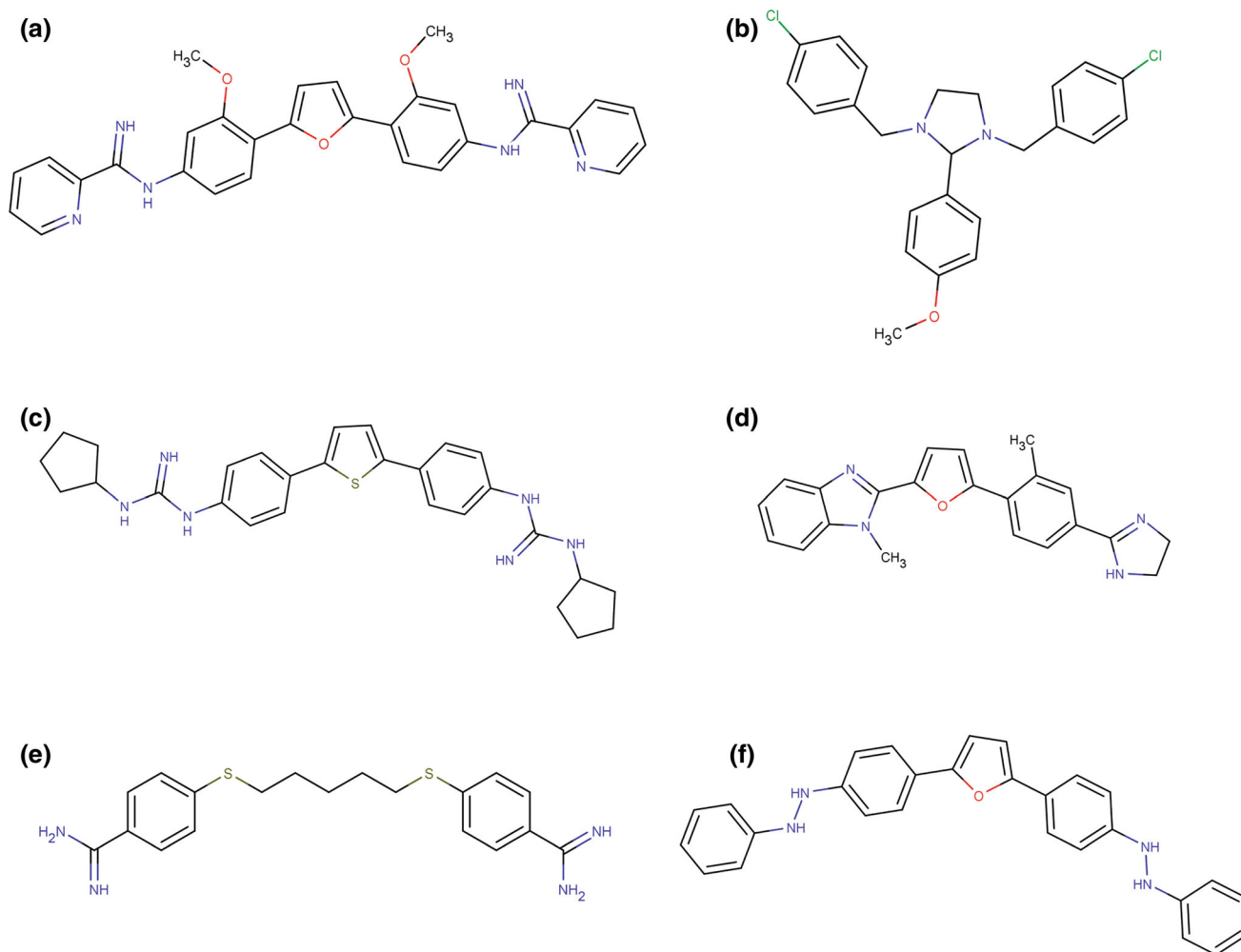


Fig. 5 Molecular structures of representative active compounds for each model: **a** model45, **b** model54, **c** model57, **d** model70, **e** model86, **f** model98

Table 1 Percentage of good classification (%GC) and AUROC for the best 6 models in the different databases

Model	Wilks' lambda	Training set		Test set		Simulated database		DUD-E library	
		% GC	AUROC	% GC	AUROC	% GC	AUROC	% GC	AUROC
98	0.58723	83	0.880*	66.7	0.742*	90.4	0.907*	74.5	0.853*
54	0.62073	81	0.862*	68	0.775*	84.8	0.887*	68.5	0.711*
70	0.60285	80	0.878*	69	0.784*	82.4	0.884*	64.8	0.641*
86	0.62168	83	0.865*	82	0.854*	88.2	0.878*	69.8	0.738*
57	0.61387	81	0.864*	72.8	0.745*	85.7	0.877*	74.5	0.766*
45	0.58662	83	0.884*	70.5	0.767*	83.8	0.876*	77.3	0.886*

Wilks' lambda is the proportion of the total variance in the discriminant scores not explained by differences among the groups. For instance, if Wilks' lambda is 0.33, it means that 33 % of the variance is not explained by group differences. Lambda varies from 0 to 1, with 0 meaning group means differ (thus the more the variable differentiates the groups), and 1 meaning all group means are the same. Thus, smaller values of Wilks' lambda are desirable.

AUROCc statistically different from a random classification * $p < 0.0001$

was allowed to develop for 20 min and then absorbance at 650 nm was measured with a MultiScan EX plate reader (Thermo Scientific). All reactions were tested in

quadruplicate. The dose–response curves were fitted to a sigmoidal Boltzmann equation. The residual activity was calculated as the mean of three independent experiments.

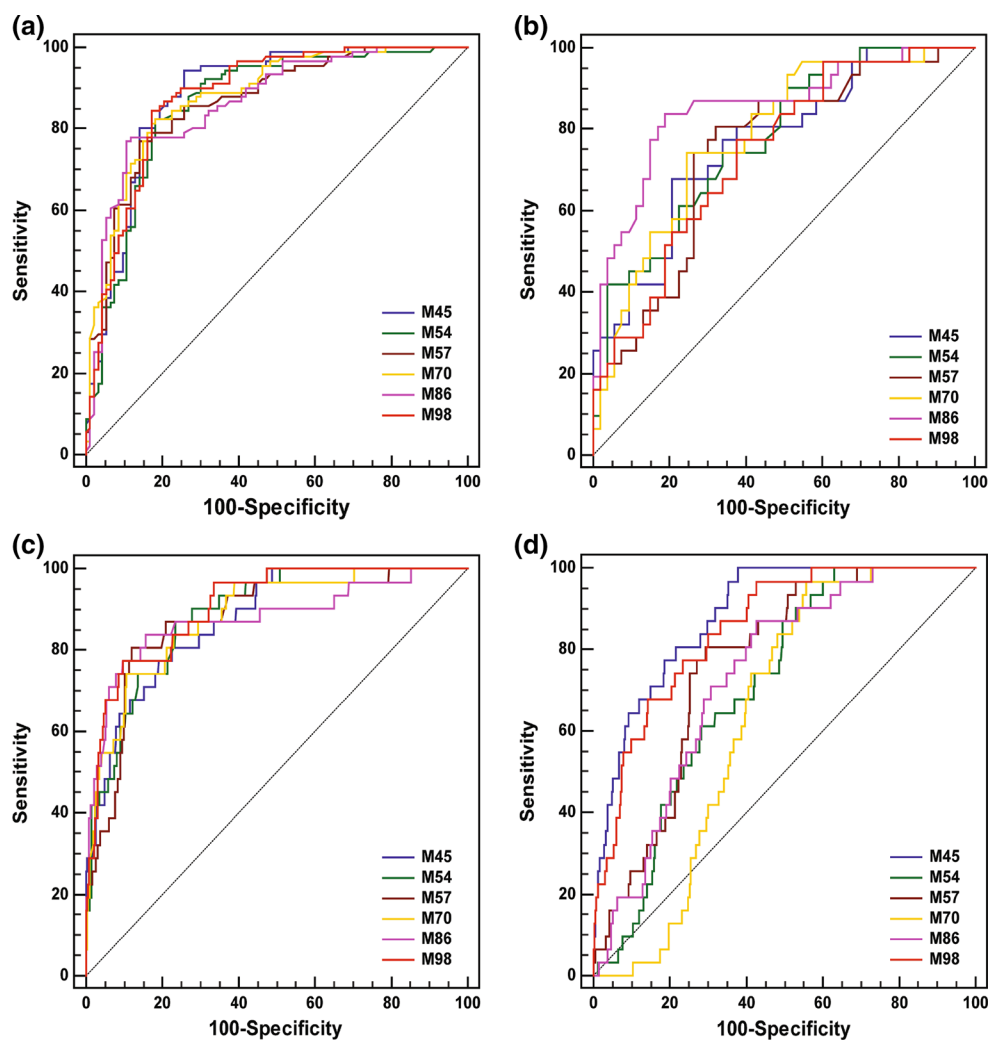


Fig. 6 Graphical comparison of the ROC curves for the 6 best performing individual models in the different databases. **a** training set, **b** test set, **c** simulated database and **d** DUD-E Library

Table 2 AUROC values of the different combinations compared with the best individual model for the different databases

	Training set	Test set	Simulated database	DUD-E library
MIN_SCORE	0.906*	0.825*	0.930*	0.927*
MODEL 98	0.880*	0.742*	0.907*	0.853*
AVERAGE_RANKING	0.913*	0.803*	0.936*	0.851*
AVERAGE_SCORE	0.916*	0.801*	0.929*	0.794*
AVERAGE_VOTING	0.793*	0.657*	0.910*	0.728*
MAX_SCORE	0.909*	0.709*	0.882*	0.530

AUROC statistically different from a random classification * $p < 0.0001$

Further details on assay and production of recombinant enzymes is provided in Sousa et al. [65] and Maiwald et al. [66].

Figure 3 shows a flowchart summarizing the strategy followed.

Results

268 polyamine analogues previously tested against *T. cruzi* were found, of which 145 were considered inactive and 123 as active. These dataset was representatively split into a

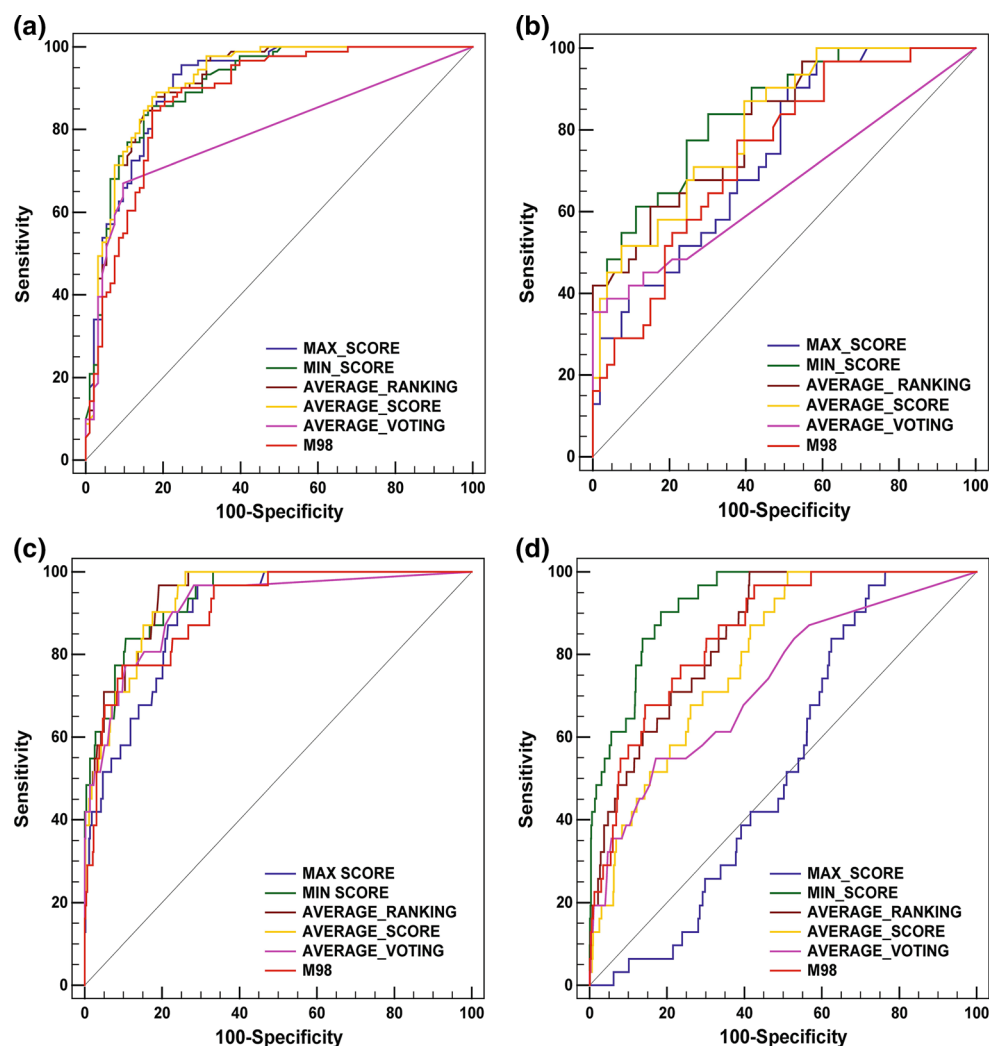


Fig. 7 Graphical comparison of the ROC curves from the best performing combinations and the best individual model (M98) in the different databases. **a** training set, **b** test set, **c** simulated database and **d** DUD-E Library

184-compound balanced training set (92 actives and 92 inactives) to infer the models and a 84-compound test set (31 actives and 53 inactives) to estimate the models' predictive ability. Figure 4 presents the heatmap illustrating the molecular dissimilarity between active and inactive compounds in the dataset, Note that there are many similar compounds (light regions) in both categories, representing a major challenge to the classification models.

We have generated 100 computational models capable of differentiating inhibitors from non-inhibitors. The following 6 models were considered the best since these presented the largest AUROC in the simulated database:

Model 45: $\text{Class} = -2.96972 + 0.01213 * \text{nCar} + 0.28881 * \text{C-034} + 0.79792 * \text{B10[C-Cl]} + 0.66370 * \text{B05[O-O]} - 1.50430 * \text{ATSC5e} + 0.15263 * \text{SM4}_{\text{Dz(Z)}} -$

$0.40497 * \text{NssNH2} - 0.03304 * \text{CATS2D}_{04_LL} + 0.06255 * \text{CATS2D}_{09_DL} + 0.33169 * \text{F04[O-O]}$

Model 54: $\text{Class} = 0.81430 + 0.00268 * \text{P_VSA}_{\text{p}_3} - 0.10301 * \text{SM14}_{\text{EA(dm)}} + 0.27199 * \text{F08[C-S]} - 1.19365 * \text{C-038} + 0.71810 * \text{B04[C-O]} + 1.11877 * \text{B10[C-S]} + 0.51879 * \text{B10[C-Cl]} - 1.41982 * \text{B06[C-C]}$

Model 57: $\text{Class} = -0.2514 + 0.0040 * \text{D/Dtr05} - 0.2842 * \text{SM03}_{\text{EA(dm)}} + 0.2881 * \text{O-060} + 0.7888 * \text{B09[C-Cl]} + 0.8274 * \text{C-019} + 0.0435 * \text{CATS2D}_{03_DL} + 0.2156 * \text{F05[C-S]} - 24.0042 * \text{JGI6}$

Model 70: $\text{Class} = -0.112964 - 0.059951 * \text{S-M15}_{\text{EA(dm)}} + 0.420284 * \text{Eig14}_{\text{EA(ri)}} - 0.222050 * \text{CATS2D}_{09_DD} + 0.324251 * \text{F01[C-S]} + 0.667668 * \text{B08[C-Cl]} + 0.012558 * \text{D/Dtr09} + 0.153316 * \text{F06[N-O]} - 0.321710 * \text{N-072}$

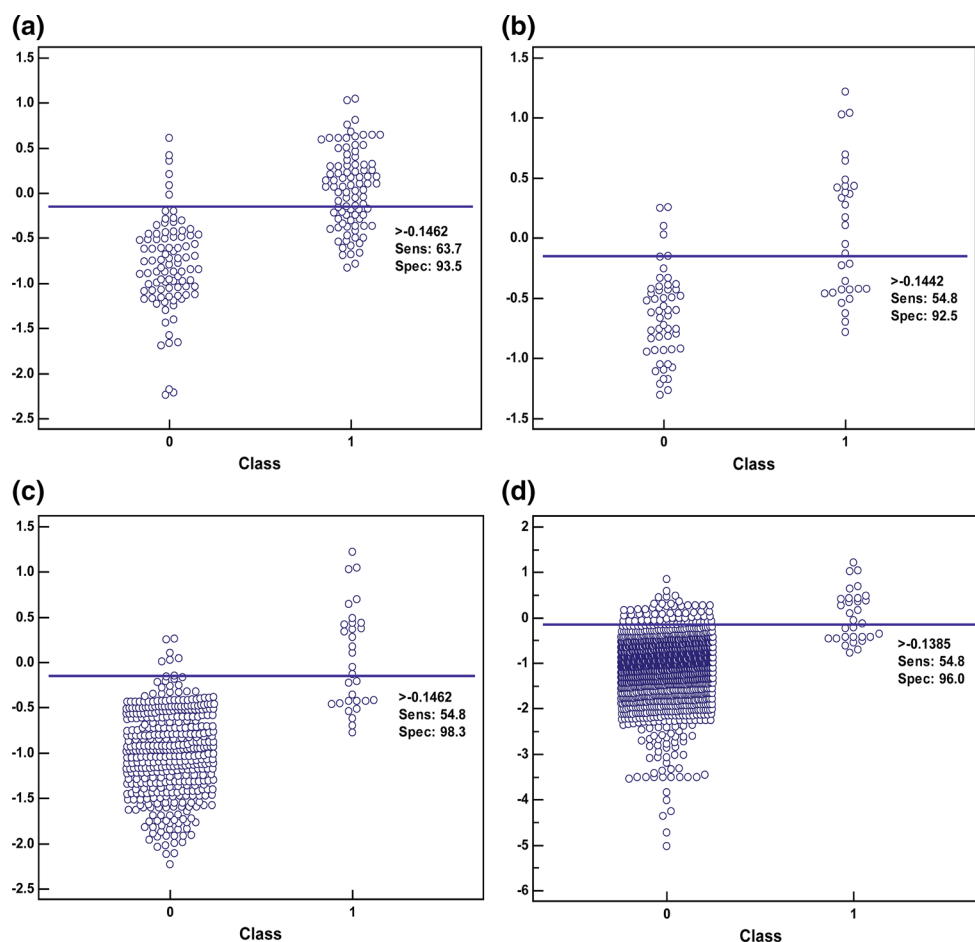


Fig. 8 Dot diagram from the MIN_SCORE in the different databases. **a** training set, **b** test set, **c** simulated database and **d** DUD-E Library

Model 86: $\text{Class} = -0.31008 + 0.23493 * \text{nCIC} - 0.73132 * \text{B05}[\text{N-N}] - 0.42672 * \text{nR} = \text{Ct} - 0.31871 * \text{SM03_EA}(\text{dm}) + 0.17102 * \text{F06}[\text{N-O}] + 36.53540 * \text{X5Av} - 1.60011 * \text{GATS1m} - 0.20345 * \text{H-048}$

Model 98: $\text{Class} = 2.27734 + 0.14469 * \text{SaasC} + 0.30672 * \text{C-034} - 0.86816 * \text{B06}[\text{C-N}] - 0.81956 * \text{J_Dz}(\text{p}) - 1.05954 * \text{GATS5s} - 0.37712 * \text{C-007} - 0.59495 * \text{B09}[\text{N-N}] - 1.42820 * \text{MATS2p}$

Figure 5 displays representative active compounds for each of the six models.

We have kept Dragon's nomenclature for the molecular descriptors. A brief description of the descriptors used by the models has been included as Supplementary Material B.

The generated models present an excellent observation/predictor ratio (around 20) which indicates a low chance of overfitting. The results for these 6 models on the training and test sets and both pilot databases are summarized in Table 1; in all cases 0 was used as score threshold to differentiate active from inactive compounds (Fig. 6).

As shown in Table 2, individual models exhibited a good performance; however, after model combination, the

performance improved significantly, which can also be observed in the ROC curves for combinations (Fig. 7). Also note that while all the combination schemes led to a similar performance on the Simulated Database, the results from the DUD-E Library (Fig. 6d) allow a better discrimination: only the MIN operator maintains the good performance previously seen in the Simulated Database (Fig. 6c). The AUROCs obtained with the MIN operator for both the Simulated Database and the DUD-E Library are virtually equal (Table 2), which is not true neither for the best individual model nor for the other combination approaches (Table 2).

The combination of models through the MIN_SCORE led to the best results in terms of Sp. This is important since a false positive is an inactive compound that the model predicts as active, and that, eventually, would be evaluated in the in vitro and cell tests giving negative results (absence of the predicted activity). Optimizing Sp is also important in our setting (public laboratory with limited funding) since the inactive compounds in the screened databases can be expected to greatly outnumber the active ones. In this way

Table 3 Acquired candidates to test experimentally

Drug	Original indication	Structure
Triclabendazole	Antiparasitic indicated to control infections of <i>Fasciola hepatica</i> and <i>Fasciola gigantica</i>	
Sertaconazole	Broad-spectrum antifungal	
Thiamine pyrophosphate	The coenzyme form of Vitamin B1 present in many animal tissues	
Eprosartan mesylate	Angiotensin II receptor antagonist used for the treatment of high blood pressure	
Paroxetine	Class of antidepressant agent known as selective serotonin-reuptake inhibitors	

we maximize the positive results in the experimental stage of evaluation, at the expense of Se.

As mentioned above, the ROC curves were analyzed to optimize the chosen threshold score on a rational basis, balancing Se and Sp according to background conditions (limited funding to conduct experimental tests, thus preferring score cutoff values associated to high Sp). Figure 8 shows a dot diagram when using the MIN_SCORE to filter each database. A score of -0.1457 in the Simulated Database was selected as the cut-off value to differentiate active from inactive compounds in the VS campaign. According to the ROC curves data, this corresponds to a sensitivity of 54.84 % and a specificity of 99.05 % in the simulated database.

The MIN_SCORE combination was then applied in the VS of the Sweetlead and DrugBank databases (more than 13,000 compounds) and 156 compounds were selected as predicted actives. 45 of these compounds are approved drugs, twelve are natural products and the remaining 99

compounds are experimental drugs. On the basis of their accessibility, five of them were acquired and experimentally tested. Nine out of 45 candidates were excluded from further analysis because they had previously been tested against *T. cruzi* (with positive results). The acquired candidates were triclabendazole (Sigma-Aldrich), sertaconazole (Sigma-Aldrich), thiamine pyrophosphate (Sigma-Aldrich), eprosartan mesylate (Sigma-Aldrich) and paroxetine (acquired from the Argentinean National Institute of Medications, INAME) (Table 3). As discussed in previous works focused on computer-guided drug repositioning [20], additional criteria to prioritize a given candidate include: (a) whether the effective concentrations on *T. cruzi* are similar to those steady state plasma concentrations attained during a multi-dosage regime for the previously approved therapeutic indication of the repositioned candidate. Preferably, equal or lower doses than those used for the original therapeutic indication should be required for our pursued indication [67]; (b) whether the repurposed

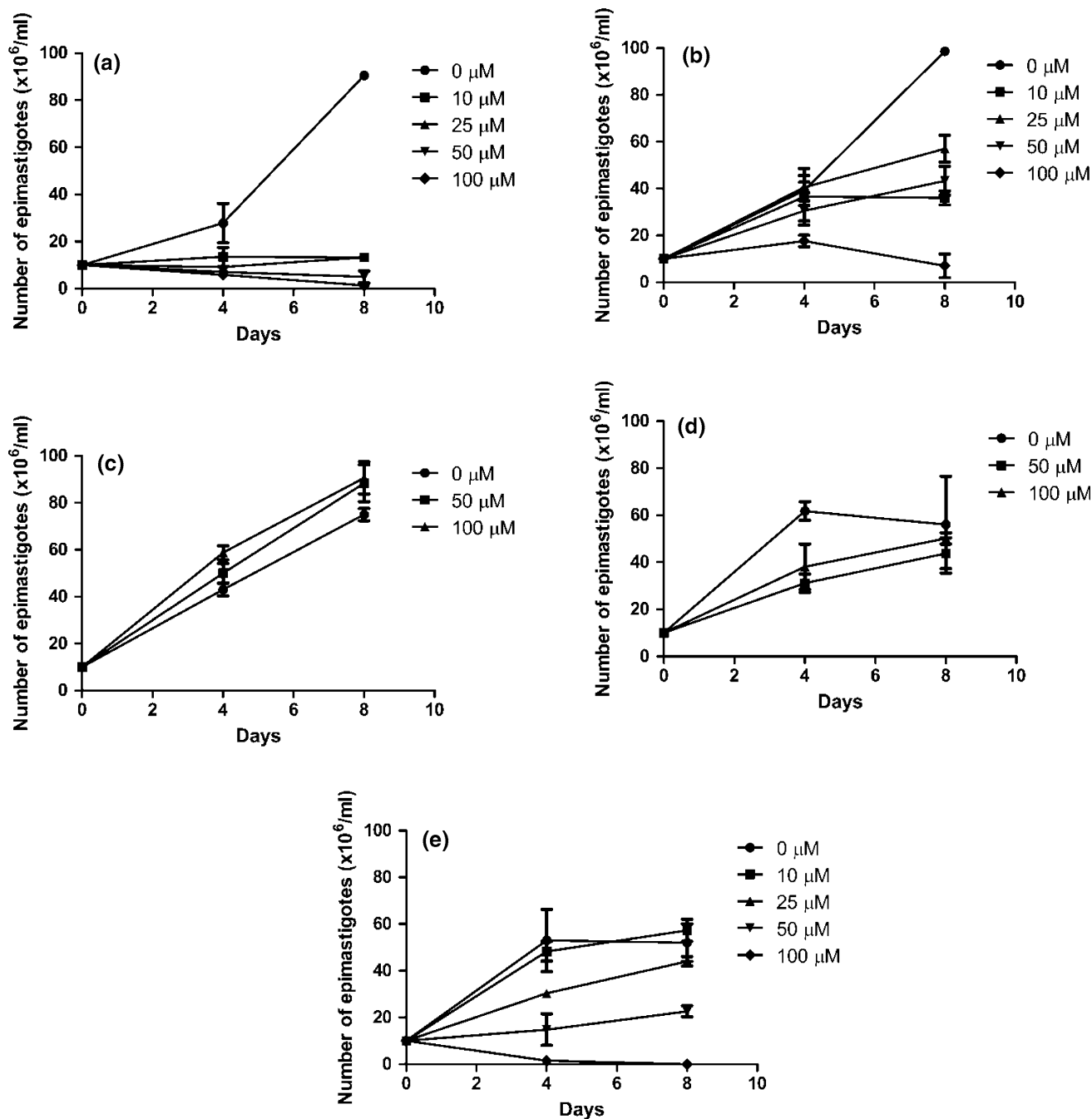


Fig. 9 Effect of the drugs on the proliferation of *T. cruzi* epimastigotes. **a** triclabendazole, **b** sertaconazole, **c** thiamine pyrophosphate, **d** eprosartan mesylate, **e** paroxetine. Results are expressed as the mean \pm SD of triplicate experiments

candidate may pose additional benefits to the patient with Chagas disease (e.g. an antichagasic agent with cardio-protective effects might help to control not only the infection but also the most frequent disease manifestation) and; (c) the severity of the known adverse effects associated to the doses used for the original indication and possible relevant contra-indications for the patient with

Chagas (e.g. cardiotoxicity). Condition a) implies that drugs administered at high doses for the original therapeutic indication (thus usually achieving higher steady state concentrations) are more directly repurposed. Triclabendazole, for instance, is very interesting from this perspective, since it is orally administered at doses between 10 and 20 mg/kg/day as a treatment for Fascioliasis. On the

Table 4 Growth inhibitory activity against pathogenic trypanosomatids

	<i>T. cruzi</i> epimastigotes (EC ₅₀ = μM)	<i>T. brucei</i> 449 bloodstream (EC ₅₀ = μM)	<i>Leishmania infantum</i> promastigotes (EC ₅₀ = μM)
Triclabendazole	4.8 ± 0.3	6.8 ± 0.2	ND ^a
Sertaconazole	53.2 ± 0.3	7.4 ± 0.2	ND ^b
Paroxetine	25.9 ± 0.1	1.2 ± 0.2	2.2 ± 0.1

ND, EC₅₀ not determined

^a At 5 μM the compound inhibited 20 % parasite proliferation

^b At 5 μM the compound inhibited 44 % parasite proliferation

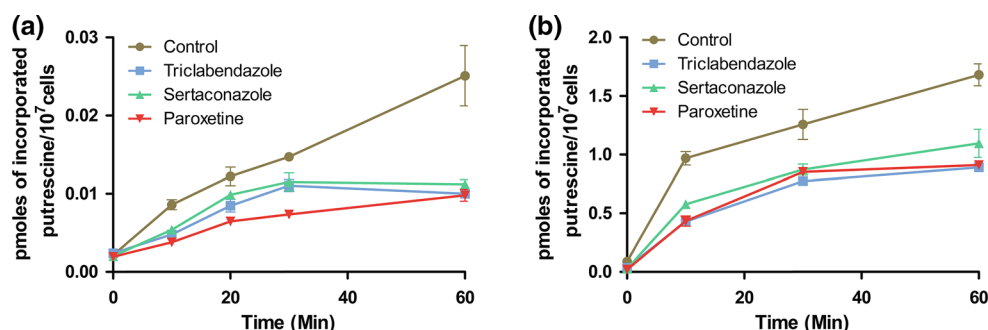


Fig. 10 Effect of the drugs on the putrescine transport for **a** *T. cruzi* wild type, **b** *T. cruzi* PAT12. Results are expressed as the mean ± SD of triplicate experiments

other hand, it has recently been reported that paroxetine reverses cardiac dysfunction in animal models of myocardial infarction, an effect that could represent an additional benefit for the patient with Chagas [68].

The biological activity of different concentrations of the candidate compounds towards *T. cruzi* epimastigotes (the proliferative and non-infective stage present in the insect vector) was tested (Fig. 9) and the EC₅₀ determined. Triclabendazole, sertaconazole and paroxetine inhibited, in a time and dose-dependent manner, the proliferation of exponentially growing parasites (day 4) with EC₅₀ values of 4.8, 53.2 and 25.9 μM, respectively (Table 4). In contrast, at the highest concentration tested (100 μM), eprosartan and thiamine pyrophosphate lacked inhibitory activity on the proliferation of *T. cruzi* (Fig. 9).

In order to determine if triclabendazole, sertaconazole and paroxetine have a broader anti-parasitic activity, the effects on the proliferation of the related pathogenic species *T. brucei* and *L. infantum* were also tested (Table 4). Whereas all three compounds displayed a one-digit μM activity against infective *T. brucei*, only paroxetine exerted an antiproliferative effect of similar potency towards *L. infantum* promastigotes (EC₅₀ = 2.2 μM for *L. infantum* vs. EC₅₀ = 1.2 μM for *T. brucei*).

In order to confirm whether the mechanism of action of the candidates correlates with that predicted by our models, the

inhibition of putrescine uptake by in a wild-type (Fig. 10a) and the PAT12 mutated strain of *T. cruzi* that overexpresses a putrescine permease [13] (Fig. 10b) was determined. All tested compounds interfered, to a similar extent, with putrescine transport from the extracellular medium.

The potential inhibitory effect of these drugs on other transporters of the same family was studied. As shown in Fig. 11, sertaconazole and triclabendazole strongly inhibited the uptake of lysine, arginine and uridine while paroxetine moderately inhibited arginine and uridine uptake and did not inhibit the incorporation of lysine. The MTT assay indicated that such short treatment (30 min) with 50 μM compounds did not affect the global energy metabolism of parasites.

Taking into account that *T. brucei* does not depend on polyamine uptake but on the de novo synthesis to fulfill their metabolic needs for polyamines [8, 69], but that all three compounds tested here were reasonable cytotoxic for infective *T. brucei*, we decided to test another potential molecular target of their anti-trypanosomal activity. TryS was selected as candidate, because this enzyme is indispensable for parasite survival and synthesizes a low molecular mass dithiol-polyamine conjugate (i.e. trypanothione) at expenses of spermidine [8]. None of the compounds displayed activity on TryS, excluding this as major target of their biological activity.

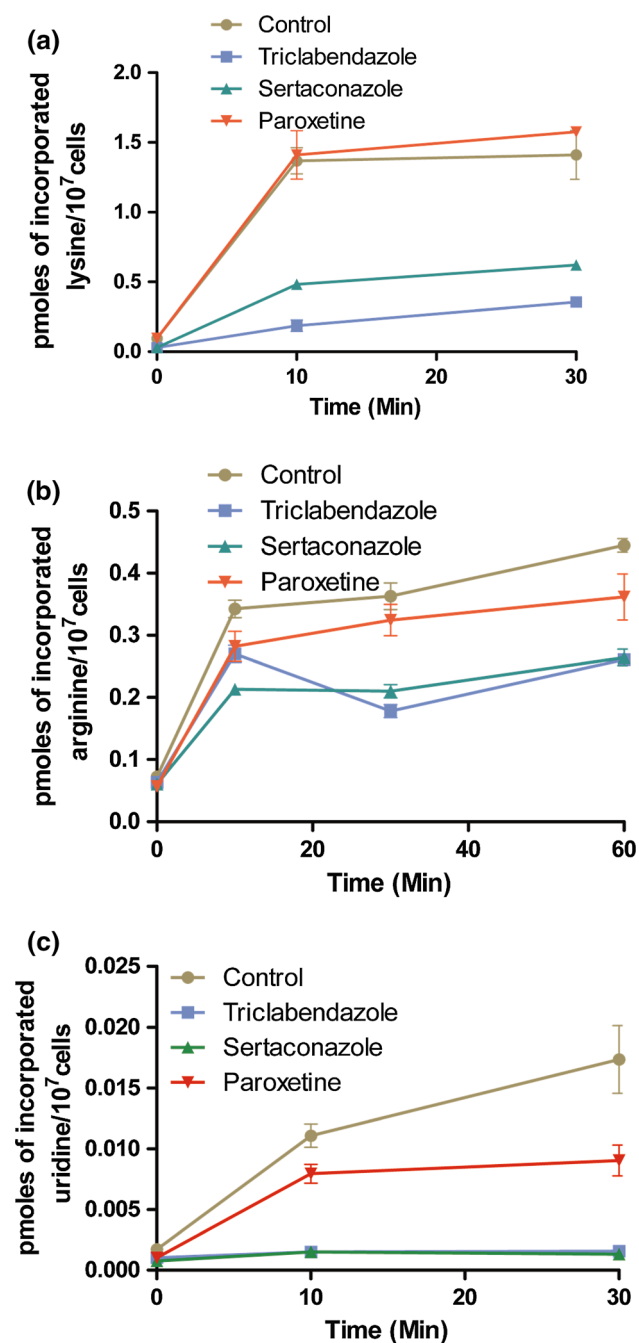


Fig. 11 Effect of the drugs on the different transports. **a** lysine transport, **b** arginine transport, **c** uridine transport. Results are expressed as the mean \pm SD of triplicate experiments

Discussion

From a database of 268 polyamine analogs previously tested against *T. cruzi*, we have generated computational models capable of discriminating between polyamine analogs with and without activity on *T. cruzi*. The models have been validated by different tests (including pilot VS campaigns on pilot databases showing low active

proportion) finding that some of them have very good predictive ability. The best models have been combined to further improve this parameter. The cut-off output score of the MIN_SCORE combination has been optimized with the help of ROC curves to increase the ensemble's Sp thus minimizing the number of false positives. We applied this model combination for the VS of Sweetlead and DrugBank databases, finding 45 approved drugs (more direct candidates to repurposing) as potential antichagasic therapies.

Among 5 candidates tested in the proliferation assay, we have found that triclabendazole inhibits the proliferation of *T. cruzi* epimastigotes at relatively low concentrations ($EC_{50} = 4.8 \mu\text{M}$); while sertaconazole and paroxetine displayed at least a fivefold lower anti-proliferative activity ($EC_{50} > 25 \mu\text{M}$). In contrast, paroxetine proved to be the most potent anti-proliferative agent against bloodstream *T. brucei* and *L. infantum* promastigotes with EC_{50} in the one-digit μM range. Although the distinct biological performance of the compounds may be ascribed to metabolic differences of the parasites stages and species studied here, it may also be possible that their mechanism of action differs between trypanosomatids. In this respect, it is worth noting that trypanosomatids fulfill their metabolic requirement of polyamines using different strategies. While *T. cruzi* is auxotroph for polyamines, *Leishmania* can either synthesize them from precursors or take them up from the extracellular medium via transporters, and African trypanosomes rely exclusively in de novo synthesis.

For *T. cruzi* epimastigotes, we could demonstrate that putrescine incorporation was affected in the presence of each of the three drugs, with the most active compounds (triclabendazole and paroxetine) showing a strong inhibition of metabolite transport that also encompassed positively charged aminoacids (lysine and arginine) or a nucleoside (uridine). Global assessment of parasite energy metabolism suggested that the decrease in transport is not due to the cytotoxicity of the drugs within the 30 min transport assay.

For *T. brucei*, TryS, a polyamine dependent and essential enzyme, was ruled out as major target of the anti-parasitic activity of the three most active compounds. Given the absence of polyamine transporters in African trypanosomes, it is very likely that triclabendazole, sertaconazole and paroxetine exert their cytotoxic activity against *T. brucei* by acting on a different molecular target and/or pathway. In this regard, future studies may address the inhibition of aminoacid/nucleoside transporters of *T. brucei* by these compounds.

It should be noted that the probability of finding an active compound from over 13,000 compounds that were screened is very low. We believe that we have validated the good predictive ability of the model combination, finding 3 active compounds out of 5 tested candidates.

The results demonstrate the utility of computational methodologies (particularly the VS of libraries of approved and experimental drugs) in the search for new therapeutic applications of known drugs. Computer-aided drug repositioning is a modern, rational and economic strategy to provide new therapeutic solutions for neglected diseases.

Acknowledgments The authors would like to thank the following public and non-profit organizations: National University of La Plata and Exact Sciences Faculty PIRPS. National University of La Plata Travel Grants and Incentivos X-730, Argentinean National Agency of Scientific and Technical Research (ANPCyT), PICT 2013-0520, CONICET. DB and MAC acknowledge the support of ANII for postgraduate fellowship (POS_NAC_2013_1_114477) and FOCEM (MERCOSUR Structural Convergence Fund, COF 03/11), respectively.

References

- Rodrigues Coura J, de Castro SL (2002) A critical review on Chagas disease chemotherapy. *Mem Inst Oswaldo Cruz* 97:3–24
- Rodrigues Coura J, Pinto Dias JC (2009) Epidemiology, control and surveillance of Chagas disease—100 years after its discovery. *Mem Inst Oswaldo Cruz* 104:31–40
- Bustamante JM, Tarleton RL (2014) Potential new clinical therapies for Chagas disease. *Expert Rev Clin Pharmacol* 7:317–325
- Nunes MC, Dones W, Morillo CA, Encina JJ, Ribeiro AL (2013) Chagas disease: an overview of clinical and epidemiological aspects. *J Am Coll Cardiol* 62:767–776
- World Health Organization (2015) Chagas disease in Latin America: an epidemiological update based on 2010 estimates. *Wkly Epidemiol Rec* 90:33–44
- Croft SL, Barret MP, Urbina JA (2005) Chemotherapy of trypanosomiasis and leishmaniasis. *TRENDS in Parasitol* 21:508–512
- Morillo CA, Marin-Neto JA, Avenzum A, Sosa-Estani S, Rassi A, Rosas F, Villena E, Quiroz R, Bonilla R, Britto C, Guhl F, Velazquez E, Bonilla L, Meeks B, Rao-Melacini R, Pogue J, Mattos A, Lazdins J, Rassi A, Connolly SJ, Yusuf S (2015) Randomized trial of benznidazole for chronic Chagas' cardiomyopathy. *N Engl J Med* 373:1295–1306
- Comini MA, Flohé L (2013) In: Flohé L, Jäger T, Koch O (eds) *Drug discovery for trypanosomatid diseases*. Oxford, Wiley
- Carrillo C, Cejas S, González NS, Algranati ID (1999) *Trypanosoma cruzi* epimastigotes lack ornithine decarboxylase but can express a foreign gene encoding this enzyme. *FEBS Lett* 454:192–196
- Carrillo C, Cejas S, Huber A, González NS, Algranati ID (2003) Lack of arginine decarboxylase in *Trypanosoma cruzi* epimastigotes. *Eukaryot Microbiol* 50:312–316
- Algranati ID, Serra MP, Carrillo C, González NS (2005) Biología molecular del metabolismo de poliaminas en parásitos tripanosomátidos. Expresión de genes heterólogos de ornitina y arginina decarboxilasa en *Trypanosoma cruzi*. *Química Viva* 2:78–94
- Carrillo C, Canepa GE, Algranati ID, Pereira CA (2006) Molecular and functional characterization of a spermidine transporter (TcPAT12) from *Trypanosoma cruzi*. *Biochem Biophys Res Commun* 334:936–940
- Hasne MP, Coppens I, Soysa R, Ullman B (2010) A high-affinity putrescine-cadaverine transporter from *Trypanosoma cruzi*. *Mol Microbiol* 76:78–91
- Pereyra CA, Carrillo C, Miranda MR, Bouvier LA, Canepa GE (2008) *Trypanosoma cruzi*: transporte de metabolitos esenciales obtenidos del hospedador. *Medicina* 68:398–404
- Comini MA, Guerrero SA, Haile S, Menge U, Lünsdorf H, Flohé L (2004) Validation of *Trypanosoma brucei* trypanothione synthetase as drug target. *Free Radic Biol Med* 36(10):1289–1302
- Sousa AF, Gomes-Alves AG, Benítez D, Comini MA, Flohé L, Jaeger T, Passos J, Stuhlmann F, Tomás AM, Castro H (2014) Genetic and chemical analyses reveal that trypanothione synthetase but not glutathionylspermidine synthetase is essential for *Leishmania infantum*. *Free Radic Biol Med* 73:229–238
- Liu Z, Fang H, Reagan K, Xu X, Mendrick DL, Slikker W Jr, Tong W (2013) In silico drug repositioning—what we need to know. *Drug Discov Today* 18:110–115
- Allarakhia M (2013) Open-source approaches for the repurposing of existing or failed candidate drugs: learning from and applying the lessons across diseases. *Drug Des Dev Ther* 2013:753–766
- Ashburn TT, Thor KB (2004) Drug repositioning: identifying and developing new uses for existing drugs. *Nat Rev Drug Discov* 3:673–683
- Bellera CL, Balcazar DE, Vanrell MC, Casassa AF, Palestro PH, Gavernet L, Labriola CA, Gálvez J, Bruno-Blanch LE, Romano PS, Carrillo C, Talevi A (2015) Computer-guided drug repurposing: identification of trypanocidal activity of clofazimine, benidipine and saquinavir. *Eur J Med Chem* 93:338–348
- Ekins S, Williams AJ, Krasowski MD, Freundlich JS (2011) In silico repositioning of approved drugs for rare and neglected diseases. *Drug Discov Today* 16:298–310
- Sbaraglini ML, Vanrell MC, Bellera CL, Benaim G, Carrillo C, Talevi A, Romano PS (2016) Neglected tropical protozoan diseases: drug repositioning as a rational option. *Curr Top Med Chem* 16
- Díaz MV, Miranda MR, Campos-Estrada C, Reigada C, Maya JD, Pereira CA, López-Muñoz R (2014) Pentamidine exerts in vitro and in vivo anti *Trypanosoma cruzi* activity and inhibits the polyamine transport in *Trypanosoma cruzi*. *Acta Trop* 134:1–9
- Silva CF, Batista MM, Alves Mota R, Mello de Souza E, Stephens CE, Som P, Boykin DW, Soeiro MNC (2007) Activity of ‘reversed’ diamidines against *Trypanosoma cruzi* ‘in vitro’. *Biochem Pharm* 73:939–946
- Liew LPP, Kaiser M, Copp BR (2013) Discovery and preliminary structure–activity relationship analysis of 1,14-sperminediphenylacetamides as potent and selective antimalarial lead compounds. *Bioorg Med Chem Lett* 23:452–454
- Da Silva CF, Da Silva PB, Batista MM, Daliry A, Tidwell RR, Soeiro MNC (2010) The biological in vitro effect and selectivity of aromatic dicationic compounds on *Trypanosoma cruzi*. *Mem Inst Oswaldo Cruz* 105(3):239–245
- Daliry A, Da Silva PB, Da Silva CF, Batista MM, De Castro SL, Tidwell RR, Soeiro MNC (2009) In vitro analyses of the effect of aromatic diamidines upon *Trypanosoma cruzi*. *J Antimicrob Chemother* 64:747–750
- Stephens CE, Brun R, Salem MM, Werbovets KA, Tanious F, Wilson WD, Boykin DW (2003) The Activity of Diguandino and ‘Reversed’ Diamidino 2,5-Diarylfurans versus *Trypanosoma cruzi* and *Leishmania donovani*. *Bioorg Med Chem Lett* 13:2065–2069
- Gonzales JL, Stephens CE, Wenzler T, Brun R, Tanious FA, Wilson WD, Barszcz T, Werbovets KA, Boykin DW (2007) Synthesis and antiparasitic evaluation of bis-2,5-[4-guandinophenyl]thiophenes. *Eur J Med Chem* 42:552–557
- De Oliveira Pacheco MG, Da Silva CF, De Souza CF, Batista MM, Da Silva PB, Kumar A, Stephens CE, Boykin DW, Soeiro MNC (2009) *Trypanosoma cruzi*: activity of heterocyclic cationic molecules in vitro. *Exp Parasitol* 123:73–80

31. Da Silva CF, Batista MM, Batista DGJ, De Souza EM, Da Silva PB, De Oliveira GM, Meuser AS, Shareef AR, Boykin DW, Soeiro MNC (2008) In vitro and in vivo studies of the trypanocidal activity of a diarylthiophene diamidine against *Trypanosoma cruzi*. *Antimicrob Agents Chemother* 52(9):3307–3314
32. Patrick DA, Ismail MA, Arafa RK, Wenzler T, Zhu X, Pandharkar T, Jones SK, Werbovetz KA, Brun R, Boykin DW, Tidwell RR (2013) Synthesis and antiprotozoal activity of dicationic m-terphenyl and 1,3-dipyridylbenzene derivatives. *J Med Chem* 56(13):5473–5494
33. Menezes D, Valentim C, Oliveira MF, Vannier-Santos MA (2006) Putrescine analogue cytotoxicity against *Trypanosoma cruzi*. *Parasitol Res* 98:99–105
34. Daliry A, Pires MQ, Silva CF, Pacheco RS, Munde M, Stephens CE, Kumar A, Ismail MA, Liu Z, Farahat AA, Akay S, Som P, Hu Q, Boykin DW, Wilson WD, De Castro SL, Soeiro MNC (2011) The trypanocidal activity of amidine compounds does not correlate with their binding affinity to *Trypanosoma cruzi* kinetoplast DNA. *Antimicrob Agents Chemother* 55(10):4765–4773
35. Birkholtz LM, Williams M, Niemand J, Louw AI, Persson L, Heby O (2011) Polyamine homeostasis as a drug target in pathogenic protozoa: peculiarities and possibilities. *Biochem J* 438:229–244
36. Lizzi F, Veronesi G, Belluti F, Bergamini C, López-Sánchez A, Kaiser M, Brun R, Krauth-Siegel RL, Hall DG, Rivas L, Bolognesi ML (2012) Conjugation of quinones with natural polyamines: toward an expanded antitrypanosomatid profile. *J Med Chem* 55(23):10490–10500
37. De Souza EM, Da Silva PB, Nefertiti ASG, Ismail MA, Arafa RK, Tao B, Nixon-Smith CK, Boykin DW, Soeiro MNC (2011) Trypanocidal activity and selectivity in vitro of aromatic amidine compounds upon bloodstream and intracellular forms of *Trypanosoma cruzi*. *Exp Parasitol* 127:429–435
38. Borges MN, Messeder JC, Figueroa-Villar JD (2004) Synthesis, anti-*Trypanosoma cruzi* activity and micelle interaction studies of bisguanilylhydrazones analogous to pentamidine. *Eur J Med Chem* 39:925–929
39. Majumder S, Kierszenbaum F (1993) Inhibition of host cell invasion and intracellular replication of *Trypanosoma cruzi* by N, N'-Bis(Benzyl)-substituted polyamine analogs. *Antimicrob Agents Chemother* 37(10):2235–2238
40. Zhu X, Liu Q, Yang S, Parman T, Green CE, Mirsalis JC, Soeiro MNC, De Souza EM, Da Silva CF, Batista DGJ, Stephens CE, Banerjee M, Farahat AA, Munde M, Wilson WD, Boykin DW, Wang MZ, Werbovetz KA (2012) Evaluation of Arylimidamides DB1955 and DB1960 as candidates against Visceral Leishmaniasis and Chagas' disease: in vivo efficacy, acute toxicity, pharmacokinetics, and toxicology studies. *Antimicrob Agents Chemother* 56(7):3690–3699
41. Klenke B, Stewart M, Barret MP, Brun R, Gilbert IH (2001) Synthesis and biological evaluation of s-triazine substituted polyamines as potential new anti-trypanosomal drugs. *J Med Chem* 44:3440–3452
42. Braga SFP, Alves EVP, Ferreira RS, Fradico JRB, Lage PS, Duarte MC, Ribeiro TG, Júnior PAS, Romanha AJ, Tonini ML, Steindel M, Coelho EF, De Oliveira RB (2014) Synthesis and evaluation of the antiparasitic activity of bis-(arylmethylidene) cycloalkanones. *Eur J Med Chem* 71:282–289
43. Caterina MC, Perillo IA, Bojani L, Pezaroglo H, Cerecetto H, González M, Salerno A (2008) Imidazolidines as new anti-*Trypanosoma cruzi* agents: biological evaluation and structure–activity relationships. *Bioorg Med Chem* 16:2226–2234
44. Perez-Lamas C, Lopez-Bigas N (2011) Gitoools: analysis and visualization of genomic data using interactive heat-maps. *PLoS One* 6:e19541
45. Stahl M, Mauser H (2005) Database clustering with a combination of fingerprint and maximum common substructure methods. *J Chem Inf Model* 45(3):542–548
46. Böcker A (2008) Toward an improved clustering of large data sets using maximum common substructures and topological fingerprints. *J Chem Inf Model* 48(11):2097–2107
47. Hariharan R, Janakiraman A, Nilakantan R, Singh B, Varghese S, Landrum G, Schuffenhauer A (2011) MultiMCS: a fast algorithm for the maximum common substructure problem on multiple molecules. *J Chem Inf Model* 51(4):788–806
48. Herhaus C (2014) Introducing fuzziness into maximum common substructures for meaningful cluster characterization. *J Cheminform* 6(Suppl 1):17
49. Talevi A, Bellera CL, Di Ianni M, Duchowicz PR, Bruno-Blanch LE, Castro EA (2012) An integrated drug development approach applying topological descriptors. *Curr Comput Aided Drug Des* 8:172–181
50. Yasri A, Hartsough D (2001) Toward an optimal procedure for variable selection and QSAR model building. *J Chem Inf Comput Sci* 41:3–6
51. Mysinger MM, Carchia M, Irwin JJ, Shoichet BK (2012) Directory of Useful Decoys, Enhanced (DUD-E): better ligands and decoys for better benchmarking. *J Med Chem* 55:6582–6594
52. Irwin JJ, Shoichet BK (2005) ZINC—a free database of commercially available compounds for virtual screening. *J Chem Inf Model* 45(1):177–182
53. Yang Y, Hongming C, Nilsson I, Muresan S, Engkvist O (2010) Investigation of the relationship between topology and selectivity for druglike molecules. *J Med Chem* 53:7709–7714
54. Yang Y, Engkvist O, Llinas A, Chen H (2012) Beyond size, ionization state, and lipophilicity: influence of molecular topology on absorption, distribution, metabolism, excretion, and toxicity for druglike compounds. *J Med Chem* 55:3667–3677
55. Triballeau N, Acher F, Brabet I, Pin JP, Bertrand HO (2005) Virtual screening workflow development guided by the “receiver operating characteristic” curve approach. Application to high-throughput docking on metabotropic glutamate receptor subtype 4. *J Med Chem* 48(7):2534–2547
56. DeLong ER, DeLong DM, Clarke-Pearson DL (1988) Comparing the areas under two or more correlated receiver operating characteristic curves: a nonparametric approach. *Biometrics* 44(3):837–845
57. Li L, Hu Q, Wu X, Yu D (2014) Exploration of classification confidence in ensemble learning. *Pattern Recogn* 47:3120–3131
58. Zhang Q, Muegge I (2006) Scaffold hopping through virtual screening using 2D and 3D similarity descriptors: ranking, voting, and consensus scoring. *J Med Chem* 49:1536–1548
59. Knox C, Law V, Jewison T, Liu P, Ly S, Frolkis A, Pon A, Banco K, Mak C, Neveu V, Djoumbou Y, Eisner R, Guo AC, Wishart DS (2011) DrugBank 3.0: a comprehensive resource for ‘Omics’ research on drugs. *NucleicAcids Res* 39:1035–1041
60. Novick PA, Ortiz OF, Poelman J, Abdulhay AY, Pande VS (2013) SWEETLEAD: an in silico database of approved drugs, regulated chemicals, and herbal isolates for computer-aided drug discovery. *PLoS One* 8(11):e79568
61. Bellera CL, Balcazar DE, Alberca LN, Labriola CA, Talevi A, Carrillo C (2013) Application of computer-aided drug repurposing in the search of New Cruzipain inhibitors: discovery of amiodarone and bromocriptine inhibitory effects. *J Chem Inf Model* 53(9):2402–2408
62. Biebinger S, Wirtz LE, Lorenz P, Clayton C (1997) Vectors for inducible expression of toxic gene products in bloodstream and procyclic *Trypanosoma brucei*. *Mol Biochem Parasitol* 85(1):99–112
63. Fernández M, Becco L, Correia I, Benítez J, Piro OE, Echeverria GA, Medeiros A, Comini M, Lavaggi ML, González M,

- Ceretto H, Moreno V, Pessoa JC, Garat B, Gambino D (2013) Oxidovanadium(IV) and dioxidovanadium(V) complexes of tridentate salicylaldehyde semicarbazones: searching for prospective antitrypanosomal agents. *J Inorg Biochem* 127:150–160
64. Mosmann T (1983) Rapid colorimetric assay for cellular growth and survival: application to proliferation and cytotoxicity assays. *J Immunol Methods* 65:55–63
65. Sousa AF, Gomes-Alves AG, Benítez D, Comini MA, Flohé L, Jaeger T, Passos J, Stuhlmann F, Tomás AM, Castro H (2014) Genetic and chemical analyses reveal that trypanothione synthetase but not glutathionylspermidine synthetase is essential for *Leishmania infantum*. *Free Radic Biol Med* 73:229–238
66. Maiwald F, Benítez D, Charquero D, Dar MA, Erdmann H, Preu L, Koch O, Hölscher C, Loaëc N, Meijer L, Comini MA, Kunick C (2014) 9- and 11-substituted 4-azapallones are potent and selective inhibitors of African trypanosoma. *Eur J Med Chem* 83:274–283
67. Oprea TI, Overington JP (2015) Computational and practical aspects of drug repositioning. *Assay Drug Dev Technol* 13(6):299–306
68. Schumacher SM, Gao E, Zhu W, Chen X, Chuprun JK, Feldman AM, Tesmer JJG, Koch WJ (2015) Paroxetine-mediated GRK2 inhibition reverses cardiac dysfunction and remodeling after myocardial infarction. *Sci Transl Med* 7(277):277ra31
69. Taylor MC, Kaur H, Blessington B, Kelly JM, Wilkinson SR (2008) Validation of spermidine synthase as a drug target in African trypanosomes. *Biochem J* 409(2):563–569